The Effect of Sand Grain Size and Salinity on the Adsorption and Viscosity of *Platostoma palustre* (Blume) A.J. Paton

Muhammad Taufiq Fathaddin[1]*, Sonny Irawan[2], Rini Setiati[1]
Pri Agung Rakhmanto[1], Suryo Prakoso[1], Andrian Sutiadi[1]
and Asri Nugrahanti[1]
[1]Department of Petroleum Engineering
Universitas Trisakti
Jakarta, 11440 Indonesia
**muh.taufiq@trisakti.ac.id*

[2]Department of Petroleum Engineering
Nazarbayev University
Nur Sultan, Kazakhstan

Date received: October 4, 2023
Revision accepted: March 18, 2026

Abstract

Platostoma palustre (Blume) A.J. Paton, a natural biopolymer, has shown promise for use in enhanced oil recovery due to its thickening properties. However, limited research has examined how environmental factors such as sand grain size and salinity affect its adsorption behavior and resulting in viscosity changes, which are key parameters in crude oil production from reservoirs. This study investigates how different sand grain sizes (0.149 mm and 0.420 mm) and salinity levels (10,000 and 20,000 ppm) influence the adsorption of P. palustre (Blume) A.J.Paton and how this adsorption affects the solution's viscosity. The biopolymer was tested in batch systems with concentrations ranging from 2,000 to 6,000 ppm. Four adsorption isotherm models: Henry, Langmuir, Freundlich, and Harkins-Jura were used to analyze adsorption behavior. Results showed that adsorption increased with smaller grain sizes and lower salinity, leading to a significant reduction in solution viscosity. Among the models, Harkins-Jura provided the best overall fit, particularly under high salinity and coarse sand conditions. These findings suggest that optimizing both the environmental conditions and polymer concentration is crucial for maximizing the performance of P. palustre (Blume) A.J. Paton in applications such as polymer flooding.

***Keywords**:* adsorption, *Platostoma palustre* (Blume) A.J. Paton, salinity, sand grain size, and viscosity

1. Introduction

Polysaccharides derived from various sources are widely used in food applications, including texture modifiers, gelling agents, stabilizers, and thickeners. One source is *Platostoma palustre* (Blume) A.J. Paton, a food plant that contains polysaccharide gum. *P. palustre* (Blume) A.J. Paton is a plant species that grows in East Asia and Southeast Asia and is better known as black grass jelly (Paton, 1997). It is a nutritious drink that is commonly served as a traditional beverage and has long been known in various regions of Indonesia. The black grass jelly drink is not only popular in Indonesia but also in other Asian countries, including China, Taiwan, Korea, Japan, Singapore, and Malaysia. Known since ancient times, black grass jelly, in addition to being a food ingredient, is also believed to have medicinal properties. Black grass jelly has been reported to be used for fever, abdominal pain (abdominal nausea), diarrhea, cough, and canker sores. It also helps prevent digestive disorders and lowers blood pressure. In South Korea, black grass jelly, which is made by adding certain spices to the mixture, is promoted as a healthy food. In China, *P. palustre* (Blume) A.J. Paton is a traditional herbal drink used as medicine (Tri *et al*., 2012; Fathaddin *et al*., 2022; Widyaningsih & Sari, 2017).

The characteristics of *P. palustre* (Blume) A.J. Paton, such as viscosity, color, and texture, have been analyzed in various concentrations and salinities (Octaviyana *et al*., 2023; Lai *et al*., 2000; Huljannah *et al*., 2020). Another important characteristic of *P. palustre* (Blume) A.J. Paton is its adsorption, since it can affect the abovementioned characteristics. Therefore, the aim of this study was to observe the adsorption of *P. palustre* (Blume) A.J. Paton on sand grains. In addition, the effect of salinity and sand grain size on adsorption and viscosity was analyzed. Several isothermal adsorption models were used to estimate the plant's adsorption patterns.

P. palustre (Blume) A.J. Paton was chosen because of its high salt tolerance, allowing it to maintain significant viscosity under a wide range of ionic conditions. Chemically, it contains a wide array of bioactive compounds, including polysaccharides, polyphenols, flavonoids, terpenoids, and sterols (Widyaningsih *et al*., 2018; Tang *et al*., 2020; Deswati *et al*., 2024). Unlike most biopolymers with random coil conformation, such as xanthan and guar, *P. palustre* (Blume) A.J. Paton exhibits rod-like behavior with lower coil overlap thresholds, allowing effective viscosity control at lower concentrations (Lai & Chao, 2000; Chao & Lai, 1999; Lai *et al*., 2000; Agi *et al*., 2020).

2. Methodology

The stages of the experiment are illustrated in Figure 1. In this research, the adsorption analysis of *Platostoma palustre* (Blume) A.J. Paton solution was carried out on sand grains. The sand was prepared with a sieve shaker (ZIA 11710 AG, Indonesia). The sizes of the sand used were 0.149 mm (100 mesh) and 0.420 mm (40 mesh). The two sand grain sizes were used to represent fine and coarse reservoir media, with the aim of evaluating how surface area affects polymer adsorption. The brine solution was made by first dissolving NaCl into distilled water using a magnetic stirrer. The salinity of the prepared brine was 10,000 ppm and 20,000 ppm. These two salinities were chosen to simulate the low-to-moderate brine concentrations typically found in oil reservoirs, as salinity affects polymer conformation, adsorption efficiency, and viscosity through electrostatic interactions and ionic strength. Then, *P. palustre* (Blume) A.J. Paton was dissolved in the brine. Solutions were prepared at concentrations of 2,000 ppm, 4,000 ppm, and 6,000 ppm. The three concentrations of polymer solutions were made for both types of brine.

Adsorption testing was carried out using the batch method (static method) (Ali & Mahmud, 2015; Abdurrazzaq *et al*., 2022) using a spectrophotometer (S-721, Visible, China). Batch methods do not take into account polymers that may be mechanically trapped (Manichand & Seright, 2014). For each experiment, sand with a 40 mesh size or 100 mesh size weighing 25 grams was put into a bottle. Then *P. palustre* (Blume) A.J. Paton solution with a concentration of 25 mL was poured into it. The bottle was stirred to ensure that the surface of all the grains of sand was well wetted with the polymer solution. The bottle was closed and stored at room temperature (30°C) for three hours to reach a state of equilibrium. After having been soaked for three hours, *P. palustre* (Blume) A.J. Paton was separated from the sand by filtering it for adsorption measurements (Fathaddin & Awang, 2004).

The final concentration was determined by measuring the absorbance. The absorbance was measured using a spectrophotometer at a wavelength of 600 nm (Ali & Mahmud, 2015; Li *et al*., 2018). Before measuring the absorbance, calibration was performed. The absorbance value was transformed into a concentration value, which is required to calculate the amount of the adsorbed polymer (Fathaddin, 2021). Then, based on the correlation between absorbance and concentration values, the final concentration could be obtained.

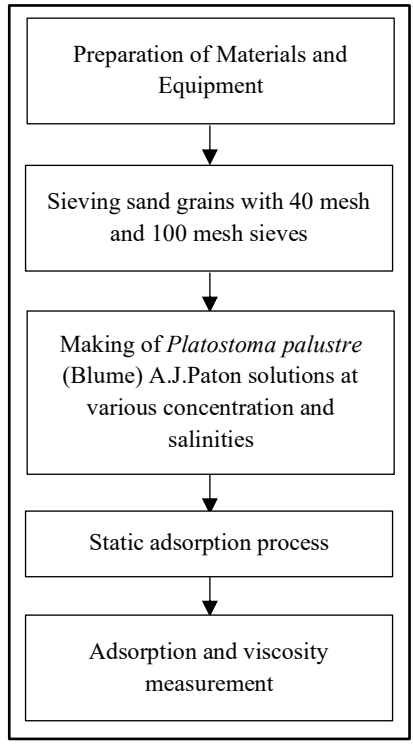

Figure 1. Stages of the experiment

The viscosity of *Platostoma palustre* (Blume) A.J. Paton was measured at room temperature using a viscometer (NDJ-8S, rotational, China). Measurements were made on the sample solution to see the effect of *Platostoma palustre* (Blume) A.J. Paton concentration and salinity on viscosity. In addition, viscosity measurements were carried out on the solution after the sand was soaked to observe the effect of adsorption on various sizes of the sand grains.

Many isothermal adsorption models have been introduced by several researchers. These can be models either for monolayer or multilayer adsorption patterns (Gilani *et al*., 2016; Ayawei *et al*., 2017; DaCosta, 2017; Alsehli, 2020; Zare *et al*., 2021). In this study, four models were used. They were Henry, Langmuir, Freundlich, and Harkin-Jura isotherm models. The Henry adsorption isotherm is generally applied to estimate the stability state of adsorption at relatively low concentration (Majd *et al*., 2021). The equilibrium concentration of adsorbate in the solution and adsorbed phase is expressed in Equation 1 (Ayawei *et al*., 2017):

$$q_e = K_{HE} C_e \quad (1)$$

where *Ce* is the adsorbate's equilibrium concentration on the adsorbent. *KHE* is Henry's adsorption constant, and *qe* is the quantity of adsorbate at equilibrium (mg/g).

The Langmuir isotherm provides surface coverage by dynamically balancing the relative rates of adsorption and desorption. The model applies to single-layer adsorption, which is limited by the assumption of uniform adsorption energy on the surface. The Langmuir equation (Equation 2) has the following linear form (Gunay *et al*., 2007; Putranti *et al*., 2017; Volesky, 2003):

$$\frac{C_e}{q_e} = \frac{1}{q_m K_L} + \frac{C_e}{q_m} \quad (2)$$

where *KL* is a Langmuir constant related to adsorption capacity (mg/g), and *qm* is maximum adsorption capacity of the adsorbent.

The Freundlich isotherm applies to adsorption processes on heterogeneous surfaces. The model can be applied to multilayer adsorption. However, if the exponent in the equation is close to 1, it can be used for monolayer adsorption. The Freundlich isotherm (Equation 3) has the following linear form (Putranti *et al*., 2017; Volesky, 2003; Ayawei *et al*., 2015; Boparai *et al*., 2011):

$$log\, q_e = log\, K_F + \frac{1}{n} log\, C_e \quad (3)$$

where *KF* represents Freundlich's adsorption capacity (L/mg) and 1/n represents adsorption intensity.

The Harkin-Jura isotherm model assumes multilayer adsorption on the surface of absorbents with heterogeneous pore distribution. The model accepts the probability of multilayer adsorption on the absorbent surface that has heterogeneous pore distribution. This model is expressed in Equation 4 (Foo & Hameed, 2010; Yokogawa *et al*., 2014; Yokogawa *et al*., 2016):

$$\frac{1}{q_e^2} = \frac{B}{A} - \left(\frac{1}{A}\right) log\, C_e \quad (4)$$

where *A* and *B* denote the Harkin-Jura constants.

The application of four isotherm models was intended to capture different adsorption behaviors. This choice allowed the researchers to comprehensively model and interpret adsorption dynamics under various environmental conditions.

3. Results and Discussion

The results of the calculation of the final concentration of *Platostoma palustre* (Blume) A.J. Paton solution with various concentrations, grain size of sand, and salinity are shown in Table 1 and Figure 2. The amount of polymer adsorbed was influenced by polymer concentration, grain size, and salinity. The tables and figures show that the adsorption rate of *P. palustre* (Blume) A.J. Paton increased with increasing concentration, decreasing particle size, and salinity.

The four isothermal adsorption models were applied to predict the adsorption. The straight-line equations of these isothermal adsorption models were used to obtain the constants of slope and intersection. The results are given in Table 2. Substitution of these constants into the original correlation form of the models was carried out to obtain the correlation between the equilibrium concentration of polymer in solution and the quantity of polymer adsorbed. This relationship is displayed in Figures 3 and 4 for a salinity of 10,000 ppm and Figures 5 and 6 for a salinity of 20,000 ppm. Each case is for the sand grain size of 0.149 and 0.420 mm, respectively. The curves shown in these figures are validated with experimental data.

Table 1. Absorbance level of *Platostoma palustre* (Blume) A.J. Paton (PP) solution

Group	Sand grain size, (mm)	Salinity, (ppm)	PP Concentration (ppm)		Adsorption (mg/g)
			Initial	Final	
	0.149	10,000	2,000	1952.5	0.076
1	0.149	10,000	4,000	3945.0	0.112
	0.149	10,000	6,000	5882.5	0.188
	0.420	10,000	2,000	1976.3	0.071
2	0.420	10,000	4,000	3962.7	0.088
	0.420	10,000	6,000	5939.0	0.183
	0.149	20,000	2,000	1992.2	0.052
3	0.149	20,000	4,000	3987.0	0.087
	0.149	20,000	6,000	5983.0	0.114
	0.420	20,000	2,000	1993.3	0.07
4	0.420	20,000	4,000	3991.0	0.095
	0.420	20,000	6,000	5987.1	0.135

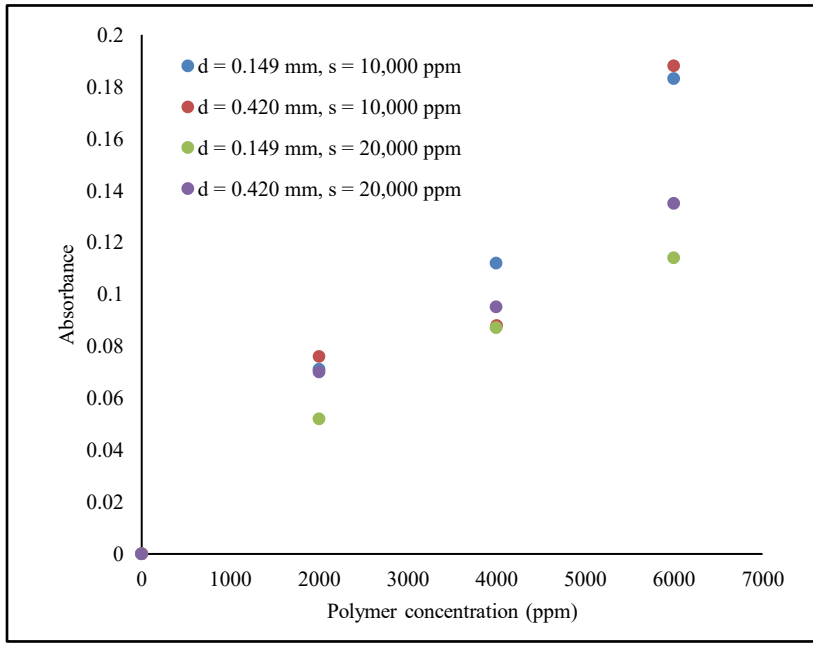

Figure 2. Absorbance curve of *Platostoma palustre* (Blume) A.J. Paton

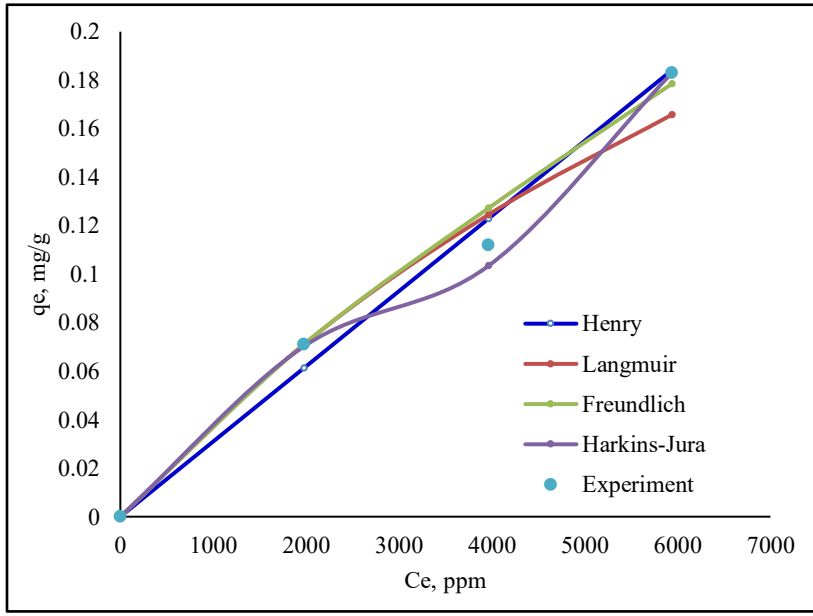

Figure 3. Experimental results and models for the *Platostoma palustre* (Blume) A.J. Paton adsorption for salinity of 10,000 ppm and grain size of 0.149 mm

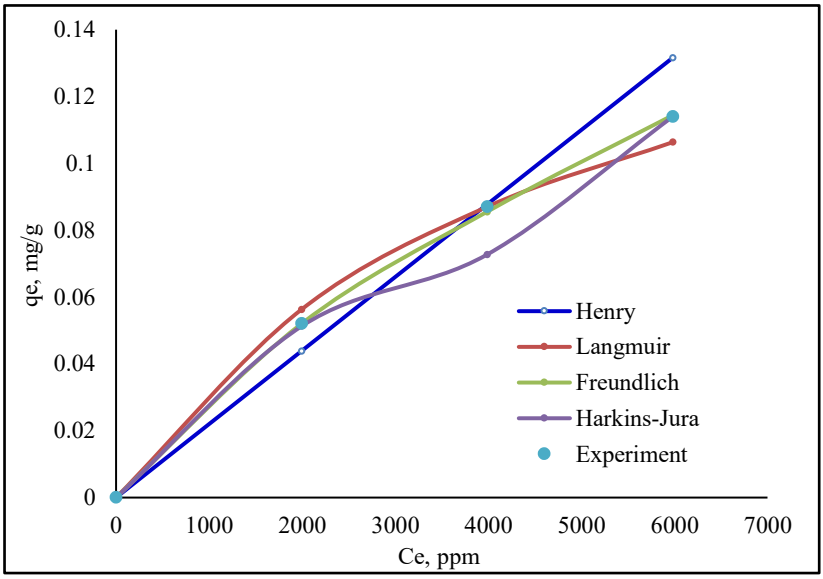

Figure 4. Experimental results and models for the adsorption of *Platostoma palustre* (Blume) A.J. Paton for a salinity of 10,000 ppm and grain size of 0.420 mm

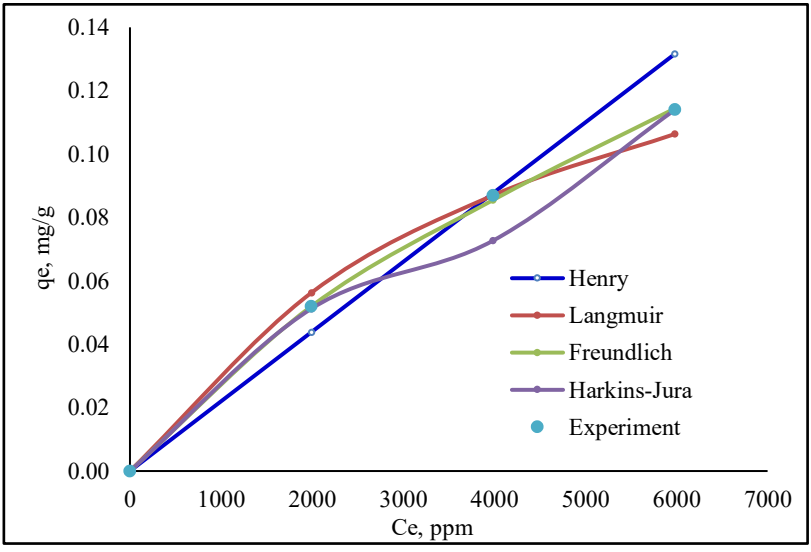

Figure 5. Experimental results and models for the *Platostoma palustre* (Blume) A.J. Paton adsorption for salinity of 20,000 ppm and grain size of 0.149 mm

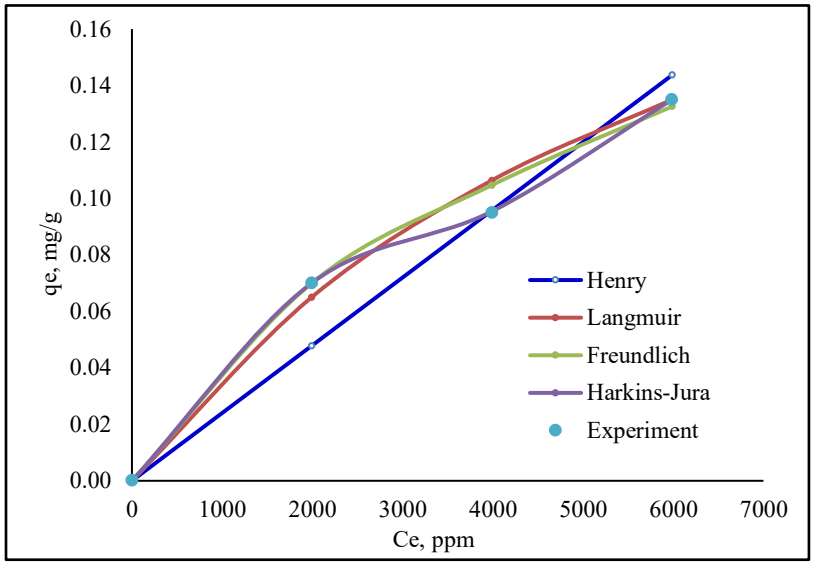

Figure 6. Experimental results and models for the *Platostoma palustre* (Blume) A.J. Paton adsorption for salinity of 20,000 ppm and grain size of 0.420 mm

Table 2. Constants of the adsorption models

Group	Sand grain size, (mm)	Salinity, (ppm)	PP Concentration (ppm)		Adsorption (mg/g)
			Initial	Final	
	0.149	10,000	2,000	1952.5	0.076
1	0.149	10,000	4,000	3945.0	0.112
	0.149	10,000	6,000	5882.5	0.188
	0.420	10,000	2,000	1976.3	0.071
2	0.420	10,000	4,000	3962.7	0.088
	0.420	10,000	6,000	5939.0	0.183
	0.149	20,000	2,000	1992.2	0.052
3	0.149	20,000	4,000	3987.0	0.087
	0.149	20,000	6,000	5983.0	0.114
	0.420	20,000	2,000	1993.3	0.07
4	0.420	20,000	4,000	3991.0	0.095
	0.420	20,000	6,000	5987.1	0.135

The relative deviation between the model and the data is expressed by the AARE parameter. The calculated AARE for the four applied correlations is illustrated in Figure 7. The AARE values for all methods varied from 0.14% to 13.48%. In general, the Harkins-Jura correlation had the lowest AARE, ranging from 0.14% to 6.94%. However, the correlation with the lowest

AARE was only in Groups 2 and 4, which was 4.66% and 0.14%, respectively. By contrast, the Freundlich correlation with the lowest AARE was in Groups 1 and 3 with 5.57% and 0.52%, respectively. Meanwhile, the strength of the relationship between the model and the measurement data was shown by all correlations. The value of the determination coefficient (r2) for all methods varied from 0.86 to 1.00, as shown in Figure 8. The Henry correlation showed the highest coefficient of determination, 0.98, for Group 1. The Harkins-Jura correlation showed the highest determination coefficient for Groups 2 (0.99) and 4 (1.00). The Freundlich correlation showed the highest coefficient of determination for Group 3 (1.00).

Table 3 shows a comparative analysis of the prediction errors (%) of four adsorption isotherm models against the experimental adsorption data. Based on the table, the performance of the isotherm models varied significantly across different experimental conditions, reflecting their capacity to interpret the adsorption mechanism and polymer-electrolyte interactions of *P. palustre* (Blume) A.J. Paton. The Harkin-Jura model consistently showed the lowest percentage errors in Groups 2 and 4 (e.g., 0.00% and 0.08%, respectively), indicating superior accuracy under high-salinity and coarse-sand conditions, where multilayer adsorption and surface heterogeneity are more pronounced. The Freundlich model exhibited the best fit in Groups 1 and 3, with 0.00% and 0.00% errors at lower salinities and finer grains, suggesting its strength in modeling heterogeneous adsorption surfaces under milder ionic conditions. In contrast, the Henry and Langmuir models showed higher errors, for instance Henry reached up to 31.66% and Langmuir up to 12.05%, particularly under conditions where their assumptions of linearity and monolayer adsorption, respectively, did not hold. These results confirm that the Harkin-Jura and Freundlich models better capture the complex adsorption behaviors influenced by both surface morphology and salinity-dependent polymer-electrolyte interactions.

Table 3. Comparison of the deviations of the estimates of the adsorption models

Group	Sand grain size, (mm)	Salinity (ppm)	Concentration (ppm)	Experiment (mg/g)	%error Henry	%error Langmuir	%error Freundlich	%error Harkins-Jura
	0.149	10,000	2,000	0.071	13.71	0.10	0.00	1.14
1	0.149	10,000	4,000	0.112	9.68	11.16	13.55	7.68
	0.149	10,000	6,000	0.183	0.61	9.42	2.46	0.00
	0.420	10,000	2,000	0.052	15.71	8.20	0.00	1.47
2	0.420	10,000	4,000	0.087	0.82	0.01	1.70	16.42
	0.420	10,000	6,000	0.114	15.46	6.72	0.36	0.00
	0.149	20,000	2,000	0.052	15.71	8.20	0.00	1.47
3	0.149	20,000	4,000	0.087	0.82	0.01	1.70	16.42
	0.149	20,000	6,000	0.114	15.46	6.72	0.36	0.00
	0.420	20,000	2,000	0.07	31.66	7.07	0.00	0.08
4	0.420	20,000	4,000	0.095	0.82	12.05	10.26	0.47
	0.420	20,000	6,000	0.135	6.44	0.03	1.81	0.00

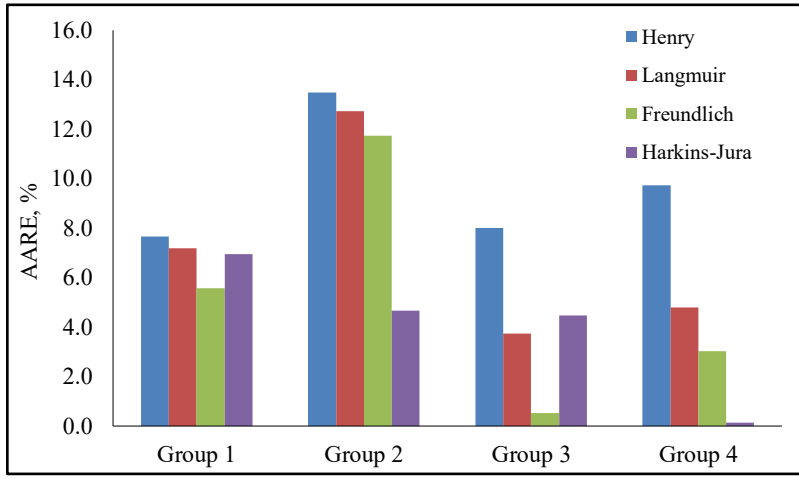

Figure 7. Average absolute relative error (AARE) of isothermal adsorption models

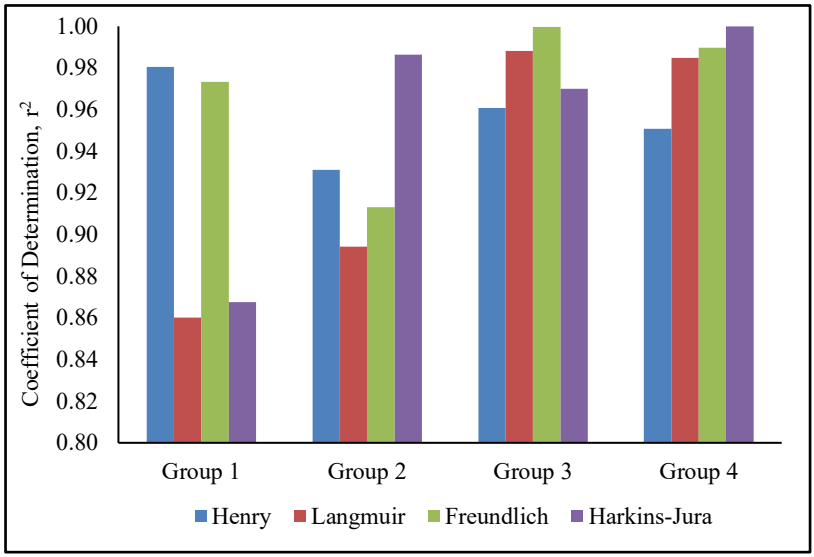

Figure 8. Coefficient of determination (r^2) of isothermal adsorption models

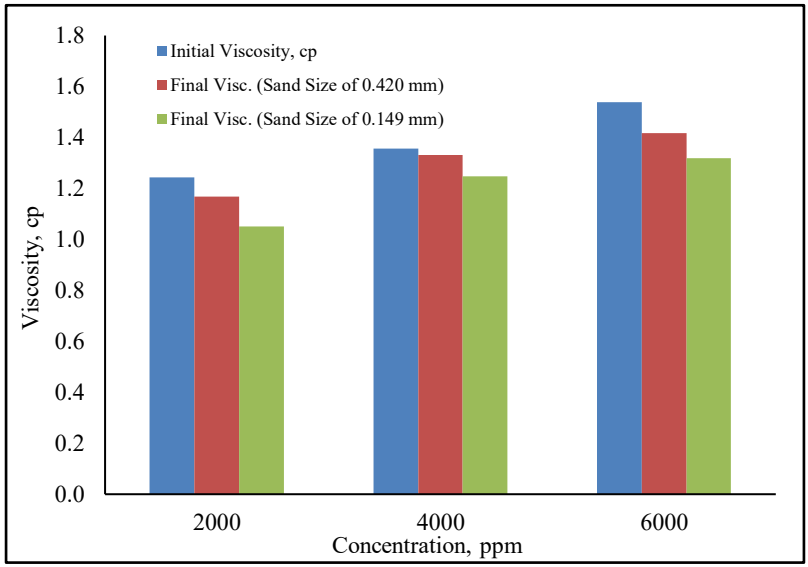

Figure 9. *Platostoma palustre* (Blume) A.J. Paton viscosity before and after adsorption at salinity of 10,000 ppm

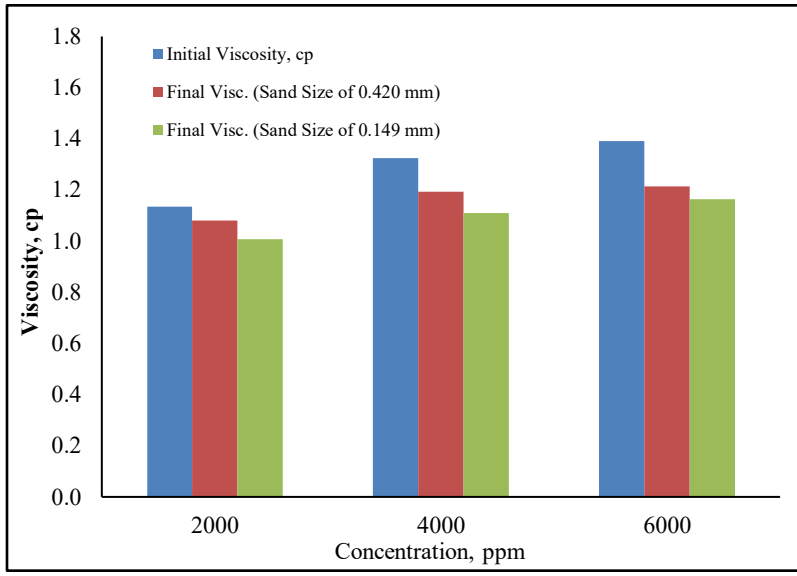

Figure 10. *Platostoma palustre* (Blume) A.J. Paton viscosity before and after adsorption at salinity of 20,000 ppm

Figures 9 and 10 show the results of viscosity measurements before and after adsorption on sand grains with a diameter of 0.149 mm and 0.420 mm at a salinity of 10,000 ppm and 20,000 ppm, respectively. Viscosity was reduced due to adsorption, where adsorption resulted in a decrease in the concentration of *P. palustre* (Blume) A.J. Paton in the solution. The observed decrease in viscosity could be attributed to the rate of adsorption. Since the amount of *P. palustre* (Blume) A.J. Paton adsorbed was affected by the size of the sand grains, a higher decrease in viscosity occurred after adsorption of the solution at a smaller sand grain size of 0.149 mm. In a solution with a salinity of 10,000 ppm, the average decrease in viscosity for grain sizes of 0.149 mm and 0.420 mm was 12.60% and 5.29%, respectively, for various concentrations of *P. palustre* (Blume) A.J. Paton. Meanwhile, for a solution with a salinity of 20,000 ppm, the average decrease in viscosity for grain sizes of 0.149 mm and 0.420 mm was 14.54% and 9.12%, respectively.

In a previous study, the viscosity reduction of shrimp chitosan also occurred due to adsorption. The average viscosity reduction of shrimp chitosan at 10,000 ppm salinity for particle sizes of 0.149 mm and 0.420 mm was 60.49% and 54.90%, respectively. Meanwhile, the average viscosity reduction of shrimp chitosan at 20,000 ppm salinity for particle sizes of 0.149 mm and 0.420 mm was 39.20% and 30.07%, respectively (Ulfah, 2023; Fathaddin *et*

al., 2024; Ulfah *et al*., 2024). Another study also examined the viscosity of crab chitosan. The average viscosity reduction of crab chitosan at 10,000 ppm salinity for particle sizes of 0.149 mm and 0.420 mm was 50.50% and 40.59%, respectively. Meanwhile, the average viscosity reduction of crab chitosan at a salinity of 20,000 ppm for particle sizes of 0.149 mm and 0.420 mm was 65.56% and 42.31%, respectively (Ulfah, 2023; Ulfah *et al*., 2023; Fathaddin, 2024). This finding indicates that the viscosity reduction of *P. palustre* (Blume) A.J. Paton due to adsorption was much lower than that of shrimp chitosan and crab chitosan. This indicates that the effect of adsorption on *P. palustre* (Blume) A.J. Paton is smaller than that of shrimp chitosan and crab chitosan. Therefore, the displacement efficiency of *P. palustre* (Blume) A.J. Paton is more stable than that of chitosan.

The increase in salinity decreased the viscosity. A possible explanation for this might be that the hydrodynamic behavior of grass jelly was influenced by ions. When the strength of the Na+ ion was low, the dominant electroviscous effect made the grass jelly molecule to have a longer and stiffer shape resulting in a higher viscosity. When the ionic strength is higher, the polymer molecules become shorter (Lai *et al*., 2000; Wicaksono & Yuliansyah, 2015). At the molecular level, salinity affects adsorption by altering electrostatic interactions and the structure of the electrical double layer at interfaces; higher ionic strength compresses this layer, reduces repulsive forces between similarly charged species, and enhances adsorption of molecules such as surfactants, polymers, or hydrocarbons onto mineral surfaces (Greathouse *et al*., 2017; Zou *et al*., 2020). Simultaneously, salinity influences viscosity through ion hydration and water structure modification; multivalent ions (e.g., Ca^{2+}, Mg^{2+}) can form hydration shells and ionic bridges that restrict molecular mobility, thereby increasing viscosity (Dastjerdi *et al*., 2024). On the other hand, larger surface area enhances adsorption by providing more active sites and increasing contact between the solute and surface, which can lead to multilayer or cooperative adsorption (Cheraghian *et al*., 2014). Additionally, high surface area materials slow down molecular motion near the interface due to confined layering and surface friction, leading to an effective increase in system viscosity. Furthermore, the salt content can also result in a decrease in the hydrodynamic volume and electrostatic repulsion of the particles which decreases the viscosity (Huljannah *et al*., 2020; Agi *et al*., 2020).

As shown in Figures 9 and 10, the average decrease in viscosity due to an increase in salinity from 10,000 ppm to 20,000 ppm was 8.88%. Previous studies showed that the decrease in viscosity due to an increase in salinity for

shrimp chitosan and crab chitosan was 38.01% and 15.36%, respectively (Ulfah, 2023; Fathaddin, 2024; Fathaddin *et al*., 2024; Ulfah *et al*., 2023; Ulfah *et al*., 2024). This shows that the effect of salinity on the viscosity of the *P. palustre* (Blume) A.J. Paton solution is much smaller than that of chitosan. Therefore, the application of the *P. palustre* (Blume) A.J. Paton solution to reservoirs with high salinity can have a more stable sweep efficiency than the application of the chitosan solution. However, because the viscosity of *P. palustre* (Blume) A.J. Paton is relatively small, it is more suitable for application in reservoirs with low oil viscosity.

4. Conclusion and Recommendation

This study examined the influence of sand grain size and salinity on the adsorption behavior and viscosity reduction of *Platostoma palustre* (Blume) A.J. Paton solutions. The results confirm that both larger grain sizes and higher salinity reduce adsorption levels, primarily due to decreased surface area and altered electrostatic interactions. The observed decrease in viscosity was directly correlated with polymer adsorption and intensified by increased salinity, which modifies molecular conformation and hydrodynamic volume.

Among the adsorption isotherm models applied, the Harkins-Jura model provided the best overall fit for Groups 2 and 4, as indicated by the lowest AARE values and highest determination coefficients (up to $r^2 = 1.00$). Meanwhile, the Freundlich model offered the most accurate predictions for Groups 1 and 3. These results highlight the importance of considering pore structure heterogeneity and surface energy distribution when modeling biopolymer adsorption on mineral surfaces.

These findings suggest that optimizing the polymer concentration applied to specific fluid salinities and reservoir rocks can minimize polymer retention and provide the best rheological behavior in practical applications, such as polymer flooding in enhanced oil recovery (EOR) processes. Future research should explore the dynamic adsorption behavior under reservoir conditions and extend the study to other biopolymers with varying ionic sensitivities and conformational characteristics.

5. Acknowledgement

This research is supported by Bima Research Grant from the Ministry of Education, Culture, Research, and Technology of the Republic of Indonesia (no. 1014/LL3/AL.04/2025) and the Research Grant from Universitas Trisakti (no. 495/A/LPPM-P/USAKTI/VI/2025).

6. References

Abdurrazzaq, A., Musa, H., & Sani, U. (2022). Sequestration of arsenate from surface water using chemically activated carbon of black velvet tamarind fruit shell. *Advanced Materials Research, 1170*, 141-154. https://doi.org/10.4028/p-77nph4

Agi, A., Junin, R., Abdullah, M.O., Jaafar, M.Z., Arsad, A., Sulaiman, W.R.W., Norddin, M.N.A.M., Abdurrahman, M., Abbas, A., & Gbadamosi, A. (2020). Application of polymeric nanofluid in enhancing oil recovery at reservoir condition. *Journal of Petroleum Science and Engineering, 194*, 107476. https://doi.org/10.1016/j.petrol.2020.107476

Ali, M., & Mahmud, H.B. (2015). The effects of concentration and salinity on polymer adsorption isotherm at sandstone rock surface. *IOP Conference Series: Materials Science and Engineering, 78*, 012038. https://doi.org/10.1088/1757-899x/78/1/012038

Alsehli, B.R.M. (2020). A simple approach for determining the maximum sorption capacity of chlorpropham from aqueous solution onto granular activated charcoal. *Process, 8*(4), 7-9. https://doi.org/10.3390/pr8040398

Ayawei, N. Angaye, S.S., Wankasi D., & Dikio, E.D. (2015). Synthesis, characterization and application of Mg/Al layered double hydroxide for the degradation of Congo red in aqueous solution. *Open Journal of Physical Chemistry, 5*(3), 56–70. http://dx.doi.org/10.4236/ojpc.2015.53007

Ayawei, N., Ebelegi, A.W., & Wankasi, D. (2017). Modelling and interpretation of adsorption isotherms. *Journal of Chemistry, 3039817*, 1-11. https://doi.org/10.1155/2017/3039817

Boparai, H.K., Joseph, M., & O'Carroll, D.M. (2011). Kinetics and thermodynamics of cadmium ion removal by adsorption onto nano zerovalent iron particles. *Journal of Hazardous Materials, 186*(1), 458–465. https://doi.org/10.1016/j.jhazmat.2010.11.029

Chao, S.J., & Lai, L.S. (1999). Effects of salt on the gelling behavior of hsian-tsao leaf gum studied using rapid-visco analyzer. *Food Science, 26*(2), 228–239. https://doi.org/10.1111/j.1365-2621.2000.tb09399.x

DaCosta, S.A. (2017). Characterization of activated carbon sample: Cu+2 adsorption isotherm. a major qualifying project, Worcester Polytechnic Institute, Worcester, United States. https://digital.wpi.edu/show/6395w8782

Deswati, D.A., Anggadiredja, K., & Garmana, A.N. (2024). Potent antioxidant activity of black grass jelly (*Mesona palustris BL*) leaf extract and fractions. *Pharmacia, 71*, 1–5. https://doi.org/10.3897/pharmacia.71.e117435

Fathaddin, M.T. (2024). The application of artificial neural network for modeling adsorption of Crab Chitosan polymer. 2024 IEEE International Conference on Artificial Intelligence and Mechatronics Systems (AIMS), Bandung, Indonesia, 2024, 1-5. https://doi.org/10.1109/AIMS61812.2024.10513085

Fathaddin, M.T., & Awang, M. (2004). Lattice gas automata simulation of adsorption process of polymer in porous media. *International Journal of Engineering Transactions A: Basics, 17*(4), 329–339. https://www.ije.ir/article_71542.html

Fathaddin, M. T. (2021). Application of isothermal model for static adsorption of xanthan gum on sandstone for various salinities. *Jurnal Offshore Oil Production Facilities and Renewable Energy*, *5*(1), 21-28. https://doi.org/10.30588/jo.v5i1.938

Fathaddin, M.T., Mardiana, D.A., Sutiadi, A., Maulida, F., & Ulfah, B.M. (2024). Modeling of shrimp chitosan polymer adsorption using artificial neural network. *Journal of Earth Energy Science Engineering and Technology, 7*(2), 37–43. https://doi.org/10.25105/jeeset.v7i2.21134.

Fathaddin, M.T., Safitri, D.U., Ridaliani, O., Widiyatni, H., Rakhmanto, P.A., Antariksa, Z.N.A., & Wijayanto, D. (2022). Educational evaluation on the benefits of clay calculation for health and beauty in the Curug Village Community, Bogor City. *Jurnal Akal Abdimas Dan Kearifan Lokal*, *3*(2), 224–230. https://doi.org/10.25105/akal.v3i2.13873

Foo, K.Y., & Hameed, B.H. (2010). Insights into the modeling of adsorption isotherm systems. *Chemical Engineering Journal, 156*(1), 2–10. https://doi.org/10.1016/j.cej.2009.09.013

Gilani, S.L., Moghadamnia, A., & Kamaruddin, A.H. (2016). Kinetics and isotherm studies of the immobilized lipase chitosan support. *International Journal of Engineering Transactions A: Basics, 29*(10), 1319–1331. https://doi.org/10.5829/idosi.ije.2016.29.10a.01

Gunay, A., Arslankaya, E., & Tosun, I. (2007). Lead removal from aqueous solution by natural and pretreated clinoptilolite: Adsorption equilibrium and kinetics. *Journal of Hazardous Materials, 146*, 362–371. https://doi.org/10.1016/j.jhazmat.2006.12.034

Huljannah, M., Lestari, F.A., & Erfando, T. (2020). Preliminary study on the utilization of seaweed and green grass jelly leaves as candidate alternatives for EOR polymer. *Teknik, 41*(3), 246-252. https://doi.org/10.14710/teknik.v41i3.28148

Lai, L. S., & Chao, S. J. (2000). A DSC study on the gel−Sol transition of a starch and Hsian-tsao leaf gum mixed system. *Journal of Agricultural and Food Chemistry*, *48*(8), 3267–3274. https://doi.org/10.1021/jf991115t

Lai, L.S., Tung, J., & Lin, P.S. (2000). Solution properties of hsian-tsao (*Mesona procumbens* Hemsl) leaf gum. *Food Hydrocolloids, 14*(3), 287–294. https://doi.org/10.1016/S0268-005X(99)00069-7

Li, Q., Pu, W., Wei, B., Jin, F., & Li, K. (2018). Static adsorption and dynamic retention of an anti- salinity polymer in low permeability sandstone core. *Journal of Applied Polymer Science, 134*(8), 44487. https://doi.org/10.1002/app.44487

Majd, M.M., Kordzadeh-Kermani, V., Ghalandari, V., Askari, A., & Sillanpää, M. (2021). Adsorption isotherm models: A comprehensive and systematic review (2010−2020). *The Science of the Total Environment*, *812*, 151334. https://doi.org/10.1016/j.scitotenv.2021.151334

Manichand, R.N., & Seright, R.S. (2014). Field vs laboratory polymer retention values for a polymer flood in the Tambaredjo field. *Society of Petroleum Engineers Journal*, SPE-169027-PA, 314-325. https://doi.org/10.2118/169027-PA

Octaviyana, H.M., Masahid, A.D., Nurhayati, N., & Fauziah, R.R. (2023). Physicochemical and organoleptic characteristics of jelly drinks with different concentrations of carrageenan, glucomannan, and fermented banana flour. *Jurnal Teknologi Pertanian*, *24*(1), 45–64. https://doi.org/10.21776/ub.jtp.2023.024.01.5

Paton, A. (1997). Classification and species of platostoma and its relationship with Haumaniastrum (*labiatae*). *Kew Bulletin, 52*(2), 257. https://doi.org/10.2307/4110385

Putranti, M.L.T.A., Wirawan, S.K., & Bendiyasa, I.M. (2017). Adsorption of free fatty acid (FFA) in low-grade cooking oil used activated natural zeolite as adsorbent. *Institute of Physics Conference Series: Materials Science and Engineering, 299*(012085). https://doi.org/10.1088/1757-899X/299/1/012085

Tang, W., Chen, X., Liu, D., & Xie, J. (2020). Bioactive components of *Mesona blume* and their potential health benefits. *Food Reviews International, 38*(sup1), 70–85. https://doi.org/10.1080/87559129.2020.1849271.

Tri, D.W., Sukardiman, Djoko, A.P., & Darmanto, W. (2012). Immunomodulatory effects of water extracts of black cincau (*Mesona palustris blume*) on carcinogenesis in mice. Jurnal *Teknologi dan Industri Pangan, 23*(1), 29-35. https://doi.org/10.6066/5290

Ulfah, B.M. (2023). Characterization and application of shrimp and crab chitosan polymers with various concentrations and salinities for oil displacement using sandpacks (MS Thesis). Universitas Trisakti, Jakarta.

Ulfah, B.M., Fathaddin, M.T., Setiati, R., Ratnaningsih, D.R., Suprayitno, A., Afifah, R. S., & Firdaus, N. (2024). Chitosan as a biopolymer in the EOR method: A literature study. *E3S Web of Conferences, 500*, 03020. https://doi.org/10.1051/e3sconf/202450003020

Ulfah, B., Setiati, R., Fathaddin, M., Ratnaningsih, Swadesi, B., Suprayitno, A., & Firdaus, N. (2023). The potential of Crab chitosan polymer as EOR injection fluid. *IOP Conference Series Earth and Environmental Science, 1239*(1), 012038. https://doi.org/10.1088/1755-1315/1239/1/012038

Volesky, B. (2003). Sorption and biosorption, Quebec, Canada: BV-Sorbex. Inc., 105–107.

Wicaksono, H., & Yuliansyah, A.T. (2015). Characterization of KYPAM HPAM polymer solution for injection material in enhanced oil recovery (EOR). *Jurnal Rekayasa Proses, 9*(1), 9–15. https://doi.org/10.22146/jrekpros.24524

Widyaningsih, T.D., & Sari, B.T.F. (2017). Antioxidant and hepatoprotective effect of black cincau (*Mesona palustris* bl) supplement against oxidative stress in rats. *International Journal of ChemTech Research, 10*(2), 45-55. https://sphinxsai.com/2017/ch_vol10_no2/abstracts/A(45-55)V10N2CT.pdf

Widyaningsih, T.D., Widjanarko, S.B., Waziiroh, E., Wijayanti, N. & Maslukhah, Y.L. (2018). Pilot plant scale extraction of black cincau (*Mesona palustris* BL) using historical-data response surface methodology. *International Food Research Journal, 25*(2), 712-719. http://www.ifrj.upm.edu.my/25%20(02)%202018/(38).pdf

Yokogawa, Y., Sano, H., Namba, S., Fujii, K., Morita, Y., Hotta, M., & Doi, Y. (2014). VSC adsorption capability of layered double hydroxide containing transition metal. *Journal of Biomimetics, Biomaterials and Biomedical Engineering, 21*, 71–74. https://doi.org/10.4028/www.scientific.net/jbbbe.21.71

Yokogawa, Y., Namba, S., Sano, H., Namba, S., Fujii, K., Morita, Y., Hotta, M., & Doi, Y. (2016), VSC adsorption capability of layered double hydroxide containing iron. *Journal of Biomimetics, Biomaterials and Biomedical Engineering, 26*, 93-96. https://doi.org/10.4028/www.scientific.net/JBBBE.26.93

Zare, H., Taleghani, H.G., & Khanjani, J. (2021). Efficient removal of copper ion from aqueous solution using crosslinked chitosan grafted with polyaniline. *International Journal of Engineering Transactions B: Applications, 34*(2), 305-312. https://doi.org/10.5829/ije.2021.34.02b.01